Stem Cell Reports
Article

ISSCR

OPEN ACCESS

CRISPR/Cas9 editing of directly reprogrammed myogenic progenitors restores dystrophin expression in a mouse model of muscular dystrophy

Seraina A. Domenig,[1] Nicola Bundschuh,[1] Ajda Lenardič,[1] Adhideb Ghosh,[1,2] Inseon Kim,[1] Xhem Qabrati,[1] Gommaar D'Hulst,[1] and Ori Bar-Nur[1,*]

[1]Laboratory of Regenerative and Movement Biology, Institute of Human Movement Sciences and Sport, Department of Health Sciences and Technology, Swiss Federal Institute of Technology (ETH) Zurich, Schwerzenbach, Switzerland
[2]Functional Genomics Center Zurich, Swiss Federal Institute of Technology (ETH) Zurich and University of Zurich, Zurich, Switzerland
*Correspondence: Ori.bar-nur@hest.ethz.ch
https://doi.org/10.1016/j.stemcr.2021.12.003

SUMMARY

Genetic mutations in *dystrophin* manifest in Duchenne muscular dystrophy (DMD), the most commonly inherited muscle disease. Here, we report on reprogramming of fibroblasts from two DMD mouse models into induced myogenic progenitor cells (iMPCs) by MyoD overexpression in concert with small molecule treatment. DMD iMPCs proliferate extensively, while expressing myogenic stem cell markers including *Pax7* and *Myf5*. Additionally, DMD iMPCs readily give rise to multinucleated myofibers that express mature skeletal muscle markers; however, they lack DYSTROPHIN expression. Utilizing an exon skipping-based approach with CRISPR/Cas9, we report on genetic correction of the *dystrophin* mutation in DMD iMPCs and restoration of protein expression *in vitro*. Furthermore, engraftment of corrected DMD iMPCs into the muscles of dystrophic mice restored DYSTROPHIN expression and contributed to the muscle stem cell reservoir. Collectively, our findings report on a novel *in vitro* cellular model for DMD and utilize it in conjunction with gene editing to restore DYSTROPHIN expression *in vivo*.

INTRODUCTION

Skeletal muscle is a soft tissue predominantly composed of multinucleated muscle fibers that contract to generate locomotion. Additionally, this tissue consists of mononucleated cells, most notably quiescent stem cells termed satellite cells, that undergo activation to regenerate the muscle tissue during growth, injury, or disease conditions (Comai and Tajbakhsh, 2014). Muscular dystrophies represent a group of over 100 diseases that inflict skeletal muscle degeneration and dysfunction as a consequence of genetic mutations in myogenic-associated genes that are important for normal muscle function. Duchenne muscular dystrophy (DMD) is an X-linked hereditary disease attributed to loss-of-function mutations in *dystrophin*, one of the largest genes in the genome (Hoffman et al., 1987; Koenig et al., 1987). Mutations in *dystrophin* manifest in progressive skeletal muscle atrophy in young boys aged 3–5 years, who oftentimes become wheelchair dependent by early adolescence and ultimately succumb to untimely death (Yiu and Kornberg, 2015). The *dystrophin* gene encodes for a structural protein, which connects the muscle cell membrane to the extracellular matrix, thus providing stabilization during muscle contractions (Dowling et al., 2021). In the absence of DYSTROPHIN, muscle contractions expedite muscle breakage accompanied by rapid cycles of degeneration and regeneration, precipitating loss of myofibers and consequently replacement with fat and fibrotic tissues over time (Dowling et al., 2021; Yiu and Kornberg, 2015).

Several therapeutic strategies have been employed to restore DYSTROPHIN expression in dystrophic muscles (Furrer and Handschin, 2019). Namely, gene editing tools such as CRISPR/Cas9 have been recently used *in vivo* and *in vitro* to restore DYSTROPHIN expression in both mouse and human muscle cells (Li et al., 2015; Long et al., 2016; Matre et al., 2019; Nelson et al., 2016; Ousterout et al., 2015; Tabebordbar et al., 2016; Young et al., 2016; Zhang et al., 2020; Zhu et al., 2017). Another approach to restore DYSTROPHIN expression in dystrophic muscles entails cell-based therapy. This method typically denotes engraftment of healthy muscle stem cells into dystrophic muscles, purposing to restore DYSTROPHIN expression via contribution of healthy myonuclei to myofibers (Domenig et al., 2020; Judson and Rossi, 2020). Freshly isolated satellite cells can efficiently engraft into dystrophic muscles, restore DYSTROPHIN expression, and contribute cells to the muscle stem cell reservoir, providing long-term regeneration competency (Kuang et al., 2007; Montarras et al., 2005; Sacco et al., 2008; Sherwood et al., 2004). However, low satellite cell extraction yield from donor-derived muscles is believed to preclude therapeutic adoption in humans (Domenig et al., 2020). Following *in vitro* expansion, satellite cells convert into highly proliferative myoblasts that exhibit a limited transplantation potential in comparison with satellite cells (Kuang et al., 2007; Montarras et al., 2005; Quarta et al., 2016; Sacco et al., 2008; Xu et al., 2015). Myoblast transplantation trials performed during the 1990s in human DMD patients reported insufficient DYSTROPHIN restoration and lack of beneficial therapeutic

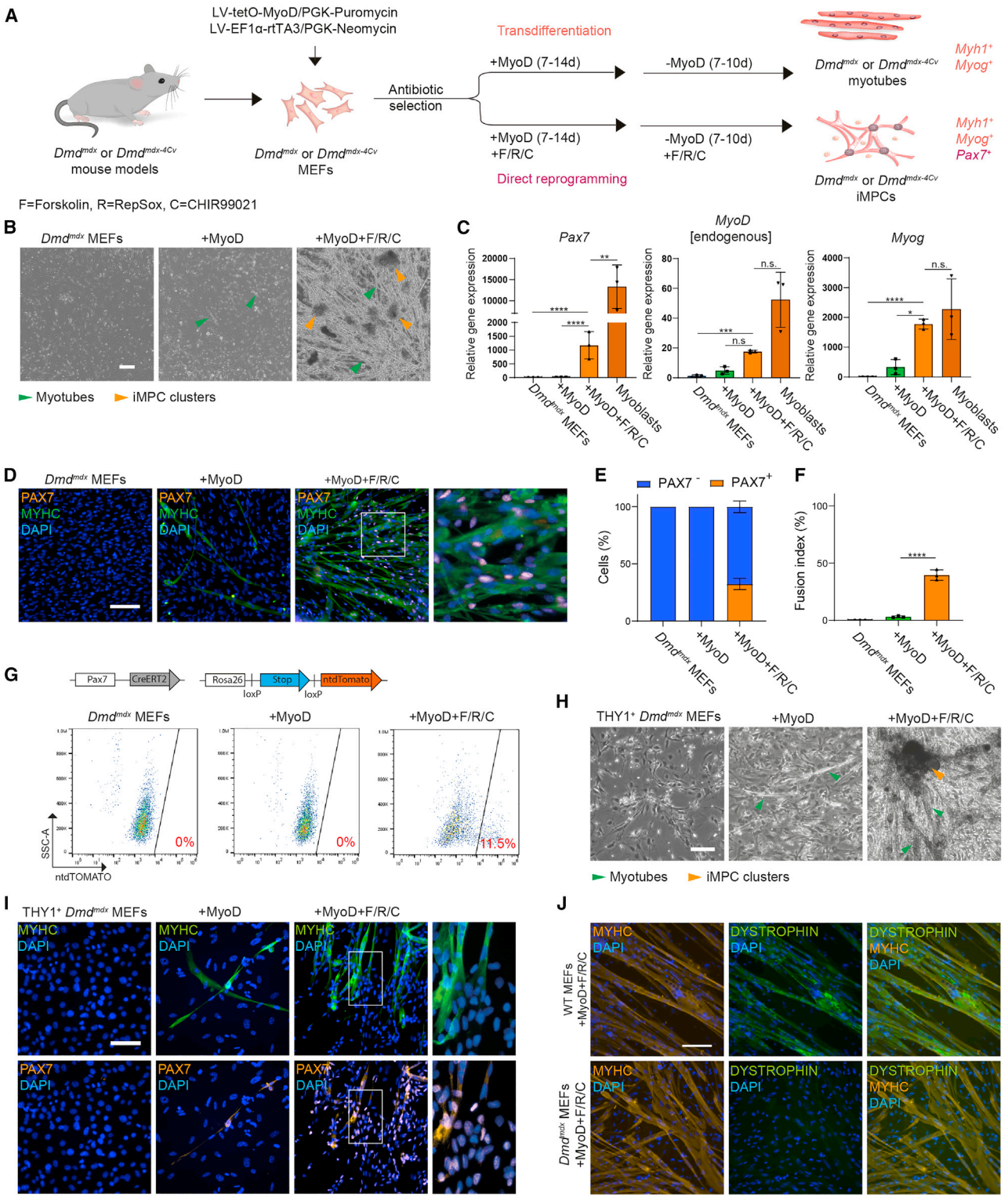

Figure 1. Direct conversion of *Dmd*^{mdx} and *Dmd*$^{mdx-4Cv}$ fibroblasts into myogenic cells

(A) An experimental outline. *Dmd*, *dystrophin* gene; MEFs, murine embryonic fibroblasts; dox, doxycycline; iMPCs, induced myogenic progenitor cells.

(B) Representative bright-field images of *Dmd*^{mdx} MEFs subjected to the indicated conditions. Scale bar, 200 μm.

(legend continued on next page)

outcome (Partridge, 2000; Skuk, 2004). This finding was attributed to poor myoblast migration in muscles, immune rejection of donor-derived cells, myoblast cell death, and lack of long-term regeneration potential of transplanted cells, albeit these reasons are still subject to extensive debate (Skuk and Tremblay, 2014).

As an alternative to satellite cells or myoblasts, pluripotent stem-cell-derived myogenic precursors have been demonstrated to efficiently engraft *in vivo* and restore DYSTROPHIN expression in DMD mouse models (Chal et al., 2015; Darabi et al., 2012; Hicks et al., 2018). However, utilizing these myogenic precursors for cell-based therapy entails a risk in the form of teratoma formation from residual pluripotent cells (Ben-David and Benvenisty, 2011). Moreover, their equivalency to embryonic muscle precursors rather than adult muscle stem cells may further render their use challenging (Xi et al., 2020).

In addition to these efforts, a recent study reported on a method to directly reprogram fibroblasts into induced myogenic progenitor cells (iMPCs) that can proliferate extensively *in vitro*, while maintaining their potential to engraft *in vivo* (Bar-Nur et al., 2018). This cellular conversion is induced by forced overexpression of the myogenic regulatory factor MyoD in conjunction with three small molecules, the cyclic AMP agonist Forskolin, the TGF-β inhibitor RepSox, and the GSK3-β inhibitor CHIR99021 (abbreviated as F/R/C). Most notably, reprogramming via this method is distinct from MyoD-mediated transdifferentiation, which converts fibroblasts into non-proliferative skeletal muscle cells (Bar-Nur et al., 2018; Davis et al., 1987). Here, we set out to investigate whether fibroblasts derived from two Duchenne mouse models can be directly reprogrammed into iMPCs that lack DYSTROPHIN expression. Furthermore, we explored means to correct the *dystrophin* mutation in DMD iMPCs *in vitro* via gene editing with CRISPR/Cas9, followed by engraftment of genetically corrected progenitors into dystrophic limb muscles, purposing to restore DYSTROPHIN expression *in vivo*.

RESULTS

MyoD in concert with small molecules elicits a myogenic stem cell identity in DMD fibroblasts

We set out to investigate whether MyoD overexpression in conjunction with small molecule treatment can generate myogenic progenitors from mouse embryonic fibroblasts (MEFs) of the Dmd^{mdx} and $Dmd^{mdx-4Cv}$ mouse models for DMD (Bulfield et al., 1984; Chapman et al., 1989). To this end, we utilized a reprogramming system, which enables wild-type (WT) fibroblast conversion into iMPCs when subjected to ectopic MyoD overexpression in concert with F/R/C treatment (Bar-Nur et al., 2018). To overexpress MyoD in Dmd^{mdx} or $Dmd^{mdx-4Cv}$ MEFs, we engineered a doxycycline (dox) inducible Tet-On lentiviral plasmid system encoding for murine MyoD under the control of a TRE3G ("Tet") promoter and a Tet3G transactivator under a constitutive EF1-α promoter (Figure 1A). Additionally, each plasmid contained an antibiotic resistance gene expressed from a constitutive mPGK promoter, thus enabling an antibiotic selection for the two cassettes in transduced MEFs (Figure 1A). Lentiviral transduction of Dmd^{mdx} or $Dmd^{mdx-4Cv}$ MEFs followed by antibiotic selection and 72–96 h of dox exposure led to abundant MYOD expression in many of the transduced cells (Figures S1A and S1B). To induce the conversion of fibroblasts into skeletal muscle cells, we exposed a similar number of transduced DMD MEFs to dox administration with or without F/R/C treatment, as previously reported for WT

(C) Quantitative real-time PCR analysis of skeletal muscle markers for the indicated conditions. Primary myoblasts served as a positive control. N = 3, each dot represents a different Dmd^{mdx} or primary myoblast cell line; error bars denote SD. Statistical analysis was performed with delta Ct values using ordinary one-way ANOVA. *$p \leq 0.05$, **$p \leq 0.01$, ***$p \leq 0.001$, ****$p \leq 0.0001$, n.s., not significant.

(D) Representative immunofluorescence images of PAX7 and MYHC in Dmd^{mdx} MEFs subjected to the indicated conditions at day 14. MYHC, myosin heavy chain. Scale bar, 100 μm.

(E) Quantification of PAX7-positive cells for the indicated conditions. Three images were taken from the same well per group and quantified. Error bars denote SD.

(F) Fusion index analysis of multinucleated muscle cells generated from Dmd^{mdx} MEFs with MyoD or MyoD+F/R/C conditions. Three images were taken from the same well per group and quantified. Error bars denote SD. Statistical analysis was performed using ordinary one-way ANOVA. ****$p \leq 0.0001$.

(G) Top: schematic of lineage tracing approach to label PAX7 expressing cells. Bottom: Flow cytometry analysis of *Pax7-CreERT2; R26-LSL-ntdTomato* Dmd^{mdx} MEFs subjected to the indicated reprogramming conditions (7 days with dox, 10 days without dox) and treated for 2 days with 4OHT at day 15.

(H) Representative bright-field images of FACS-purified $THY1^+$ Dmd^{mdx} MEFs subjected to the indicated conditions at day 21. Scale bar, 200 μm.

(I) Representative immunofluorescence images of PAX7 and MYHC-positive cells that were directly converted from FACS-purified $THY1^+$ Dmd^{mdx} MEFs with MyoD or MyoD+F/R/C treatment. Scale bar, 100 μm.

(J) Representative immunofluorescence images of DYSTROPHIN and MYHC in WT and Dmd^{mdx} MEFs at day 28 of MyoD+F/R/C treatment. Scale bar, 100 μm.

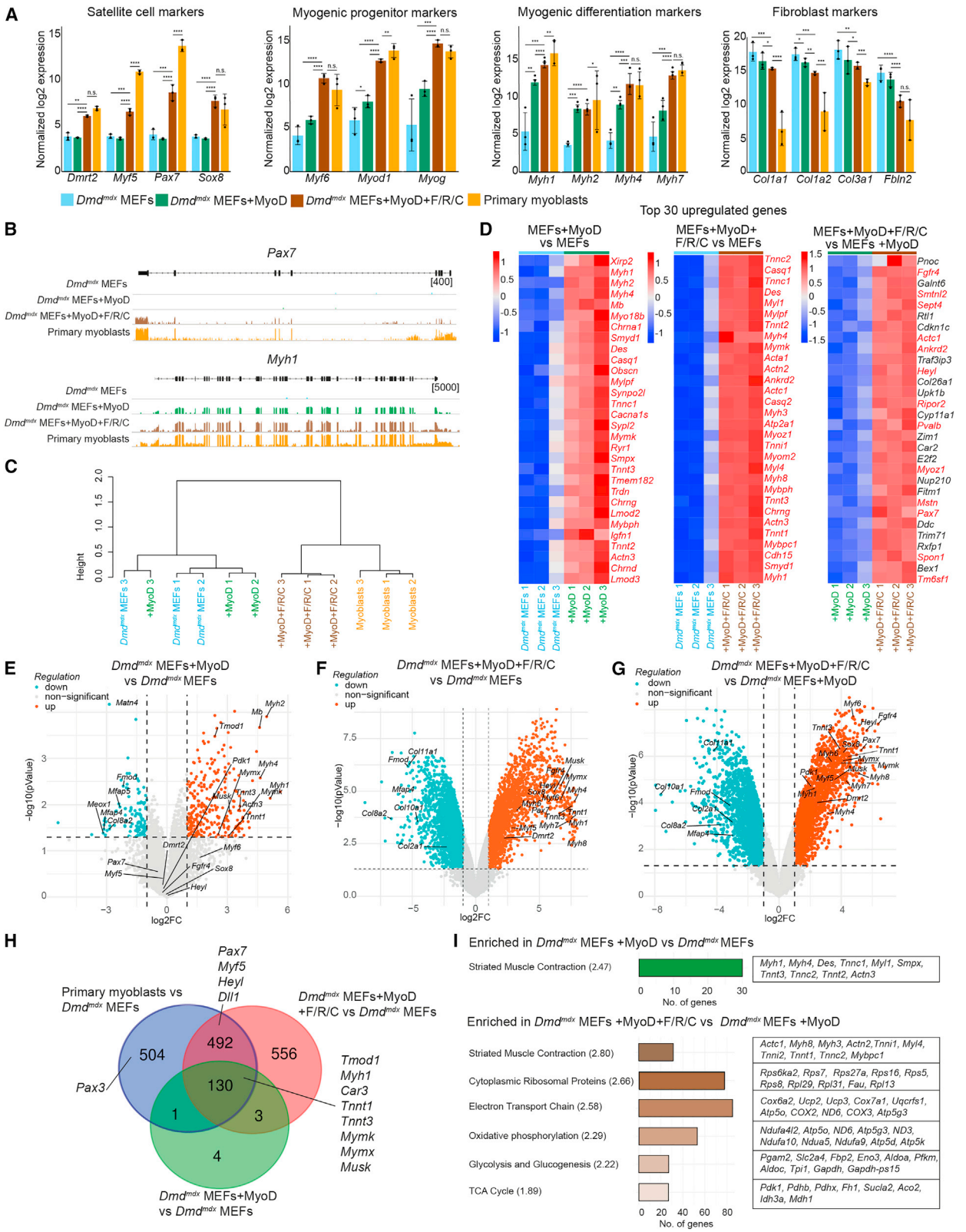

(legend on next page)

MEFs (Bar-Nur et al., 2018). Following several days of sustained MyoD overexpression, fibroblasts gave rise to multinucleated myotubes in both conditions (Figure 1B and S1C). However, in the MyoD+F/R/C condition, the myotubes were larger in size and highly contractile, and we further documented three-dimensional cell clusters and small mononucleated cells that resembled iMPCs (Figure 1B and S1C; Video S1) (Bar-Nur et al., 2018). To assess whether F/R/C treatment facilitated the formation of myogenic progenitors, we performed quantitative real-time PCR at days 14–17 for canonical myogenic stem and differentiated cell markers and documented robust upregulation of the muscle stem cell marker *Pax7* only in the MyoD+F/R/C condition, whereas endogenous *MyoD* and the differentiation marker *Myog* were upregulated in both conditions (Figure 1C). To corroborate this observation at the protein level, we immunostained these cultures for MYHC and PAX7 and detected multinucleated MYHC$^+$ myotubes in both MyoD and MyoD+F/R/C conditions; however, clusters of PAX7$^+$ cells were only detected in MyoD+F/R/C (Figures 1D, 1E, and S1D). Of note, the fusion index of MYHC$^+$ myofibers generated via MyoD+F/R/C condition was significantly higher in comparison with myotubes generated via MyoD overexpression alone (Figure 1F). Furthermore, we reprogrammed transgenic *Dmd*^{mdx} MEFs that harbored a *Pax7-CreERT2; Rosa-LoxSTOPLox(LSL)-ntdTomato* reporter for muscle stem cells (Murphy et al., 2011). Notably, we observed the formation of ntdTOMATO$^+$ cells only in fibroblasts subjected to the MyoD+F/R/C condition (Figures 1G and S1E).

Next, to exclude the possibility that F/R/C treatment promoted the proliferation of myogenic progenitors present in MEF cultures, we fluorescence-activated cell sorting (FACS)-purified *Dmd*^{mdx} MEFs using the surface marker THY1 (Polo et al., 2012). We detected 73% THY1$^+$ *Dmd*^{mdx} MEFs and sorted these fibroblasts for subsequent reprogramming experiments (Figure S1F). FACS-purified THY1$^+$ *Dmd*^{mdx} fibroblasts were subjected to MyoD or MyoD+F/R/C conditions and gave rise to multinucleated MYHC$^+$ myotubes in both conditions, whereas PAX7$^+$ iMPC-like clusters were only detected using MyoD+F/R/C (Figures 1H and 1I). Importantly, multinucleated myofibers reprogrammed from WT fibroblasts expressed both MYHC and DYSTROPHIN, whereas MYHC$^+$ myofibers reprogrammed from *Dmd*^{mdx} MEFs did not (Figure 1J). Collectively, these findings establish that DMD fibroblasts can be directly converted into PAX7$^+$ myogenic progenitors and myofibers when subjected to MyoD+F/R/C treatment, whereas MyoD overexpression alone solely generates multinucleated myotubes. Furthermore, myofibers reprogrammed from DMD fibroblasts did not express DYSTROPHIN, thus capturing disease phenotype *in vitro*.

Transcriptional dynamics during myogenic conversion of *Dmd*^{mdx} fibroblasts

To gain further insights into the genes and pathways that are upregulated or downregulated during iMPC formation, we performed bulk RNA sequencing (RNA-seq) of parental *Dmd*^{mdx} MEFs, *Dmd*^{mdx} MEFs subjected to MyoD or MyoD+F/R/C conditions (14-17 days), and primary myoblasts. We observed that exposure of *Dmd*^{mdx} MEFs to MyoD+F/R/C treatment robustly upregulated satellite cell markers (*Pax7*, *Myf5*, *Dmrt2*, and *Sox8*), which were not detected in MyoD overexpression alone (Figure 2A). Moreover, committed myogenic progenitor and early differentiation markers (*Myog*, endogenous *MyoD*, and *Myf6*) were significantly more upregulated in the MyoD+F/R/C versus MyoD condition (Figure 2A). As expected, myogenic differentiation markers (*Myh1*, *Myh2*, and *Myh4*) were upregulated in both conditions; however, fibroblast-specific genes were significantly more downregulated following MyoD+F/R/C

Figure 2. Transcriptome analysis following myogenic conversion of *Dmd*^{mdx} fibroblasts

(A) Gene expression analysis at day 14–17 based on bulk RNA-seq for the indicated conditions. N = 3, each dot represents a different cell line; error bars denote SD, *p $\leq$ 0.05, **p $\leq$ 0.01, ***p $\leq$ 0.001, ****p $\leq$ 0.0001, n.s. not significant.

(B) Integrative Genomic Viewer (IGV) tracks for *Pax7* and *Myh1*. Data range for each sample is shown using a logarithmic scale.

(C) Dendrogram based on normalized bulk RNA-seq data showing hierarchical clustering of all samples using the 2,000 genes with the highest variance. N = 3 different cell lines.

(D) Heatmap showing clustering of the top 30 most upregulated genes for the indicated comparisons. Myogenic-associated genes are highlighted in red. Each sample represents a different *Dmd*^{mdx} cell line. Gradient of high to low gene expression relative to the average expression is indicated by red to blue colors.

(E) Volcano plot based on RNA-seq data demonstrating DEGs between the indicated samples. An average of 3 different cell lines was used for each group. p value < 0.05; |log2FC| > 1.

(F) Volcano plot based on RNA-seq demonstrating DEGs between the indicated samples. An average of 3 different cell lines was used for each group. p value < 0.05; |log2FC| > 1.

(G) Volcano plot based on RNA-seq data demonstrating DEGs between the indicated samples. An average of 3 different cell lines was used for each group. p value < 0.05; |log2FC| > 1.

(H) Venn diagram for upregulated genes (>2-fold or more relative to *Dmd*^{mdx} MEFs, p < 0.05) in the indicated samples. An average of N = 3 different cell lines was used for each group.

(I) Significant functional annotations using the Wikipathway database. Normalized enrichment scores are indicated in brackets.

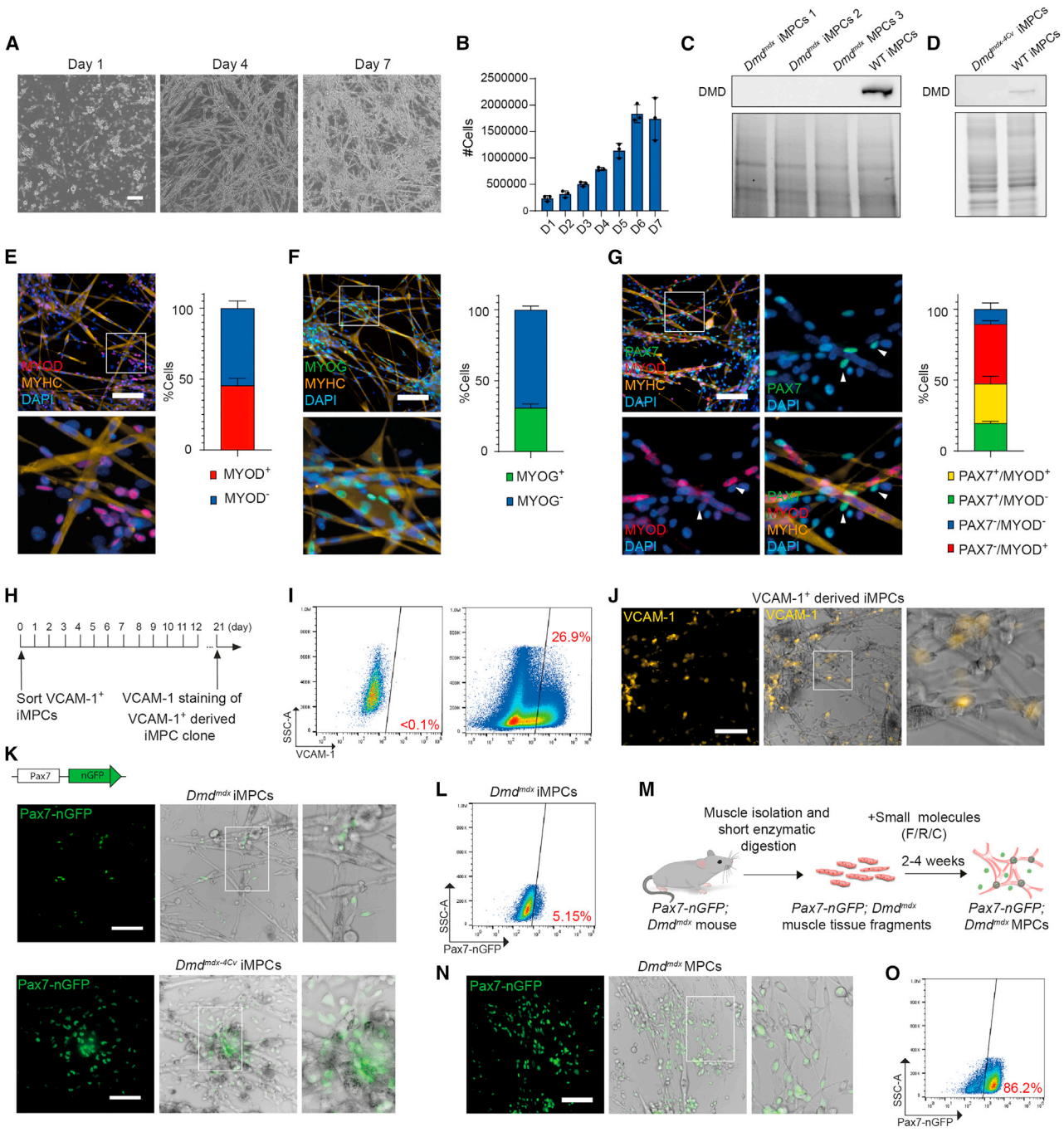

Figure 3. DMD iMPCs expand long term *in vitro*, while expressing key myogenic genes

(A) Bright-field images of a stable *Dmd*^{mdx} iMPC clone during 7 days. Scale bar, 200 μm.

(B) Graph showing a growth curve of *Dmd*^{mdx} iMPCs. Each dot represents and independent experiment using the same cell line. Error bars denote SD.

(C) Western blot for DYSTROPHIN expression in the indicated cell lines.

(D) Western blot for DYSTROPHIN expression in *Dmd*$^{mdx-4Cv}$ iMPCs and WT iMPCs.

(E) Representative immunofluorescence images for MYOD and MYHC in stable *Dmd*^{mdx} iMPCs at passage 8 and quantification. Error bars denote SD, scale bar, 100 μm.

(F) Representative immunofluorescence images of MYOG and MYHC in a stable *Dmd*^{mdx} iMPC clone at passage 9 and quantification. Error bars denote SD, scale bar, 100 μm.

(legend continued on next page)

treatment (Figures 2A and 2B). Of note, we confirmed the presence of the *dystrophin* mutation at exon 23 in *Dmd* mRNA transcripts of two *Dmd*^{mdx} MEF lines subjected to MyoD+F/R/C condition; however, we did not detect it in a third MEF line (Figure S2A).

Next, we performed unsupervised hierarchical clustering based on normalized RNA-seq data and determined that *Dmd*^{mdx} MEFs subjected to MyoD+F/R/C clustered more closely with primary myoblasts and separately from *Dmd*^{mdx} MEFs and *Dmd*^{mdx} MEFs+MyoD condition (Figures 2C and S2B). Given this observation, we investigated the significant upregulated genes in each of the reprogramming conditions. We first generated heatmaps based on the top 30 most upregulated genes in MyoD or MyoD+F/R/C condition in comparison with parental *Dmd*^{mdx} MEFs (Figure 2D). This analysis uncovered a large cohort of skeletal muscle differentiation markers (*Myh1*, *Myh4*, *Casq1*, *Chrnd*, *Des*, and *Ryr1*), which were upregulated following MyoD or MyoD+F/R/C conditions (Figure 2D). However, a comparison of the top 30 most upregulated genes in MyoD+F/R/C versus MyoD condition revealed genes that were indicative of satellite cells (*Pax7*, *Heyl*, and *Fgfr4*) as well as unique skeletal muscle differentiation genes (*Myoz1* and *Mstn*) (Figure 2D). Furthermore, a global analysis of the most differentially expressed genes (DEGs) demonstrated that MyoD overexpression did not upregulate differentiation markers to the same extent as MyoD+F/R/C condition, whereas upregulation of muscle stem cell markers was solely detected in MyoD+F/R/C condition (Figures 2E and 2F). Comparison of MyoD+F/R/C versus MyoD conditions revealed stem cell markers (*Pax7*, *Heyl*, *Myf5*, *Dmrt2*, *Sox8*, and *Fgfr4*) and muscle differentiation markers (*Tnnt1*, *Tnnt3*, *Myf6*, *Mymk*, *Mymx*, and *Musk*) that were solely or significantly more expressed in the MyoD+F/R/C versus MyoD condition (Figure 2G).

To further corroborate these results, we identified the upregulated genes (2-fold or more, p value < 0.05) for primary myoblasts, MyoD+F/R/C, or MyoD conditions in comparison with *Dmd*^{mdx} MEFs. Whereas several skeletal muscle differentiation markers were upregulated in all three cell types versus fibroblasts, stem cell markers such as *Pax7*, *Myf5*, and *Heyl* were only enriched in primary myoblasts and the MyoD+F/R/C condition (Figure 2H). Accordingly, a pathway enrichment analysis of ranked genes based on log2FC between MyoD+F/R/C versus MyoD or MyoD versus MEFs revealed categories associated with "striated muscle contraction" for both comparisons. However, a comparison of MyoD+F/R/C versus MyoD conditions revealed multiple enriched gene categories associated with enhanced metabolic activity (glycolysis, oxidative phosphorylation, and TCA cycle) (Figure 2I). In summary, the transcriptome analysis highlighted the pronounced upregulation of myogenic stem cell genes and unique skeletal muscle differentiation markers only in MyoD+F/R/C condition. These transcriptional changes are on par with the robust proliferation and contractility observed in MyoD+F/R/C reprogrammed cultures and suggest enhanced capture of skeletal muscle cell identity *in vitro*.

DMD iMPCs proliferate extensively while expressing stem cell and differentiation genes

Our observation that *Dmd*^{mdx} and *Dmd*$^{mdx-4Cv}$ MEFs exposed to MyoD+F/R/C treatment can give rise to a population of proliferative progenitor cells prompted us to attempt expanding dox-independent DMD iMPC lines. To this end, three-dimensional colonies were passaged and propagated in medium containing F/R/C and in the absence of dox. Following 1–2 days after cell splitting, mononucleated cells were predominantly detected in the culture dish; however, many of these cells proliferated or fused within a week, giving rise to the entire contractile network of multinucleated muscle fibers and mononucleated cells (Figures 3A and 3B; Video S2). Importantly, established *Dmd*^{mdx} as well as *Dmd*$^{mdx-4Cv}$ iMPC lines did not express DYSTROPHIN protein in comparison with WT iMPCs; however, they robustly expressed stem, progenitor, and differentiation cell markers (Figures 3C–3G and S3A). Of note, by co-immunostaining *Dmd*^{mdx} iMPCs for PAX7, MYOD, and MYHC, we detected PAX7^{+}/MYOD^{-} mononucleated cells, suggesting that stable DMD iMPCs contain immature muscle stem cells (Figure 3G).

The presence of PAX7^{+} progenitors in *Dmd*^{mdx} iMPCs prompted us to search for means to purify the progenitor cell fraction from the heterogeneous iMPC cultures. We first analyzed *Dmd*^{mdx} iMPCs by Flow cytometry for the

(G) Representative immunofluorescence images of PAX7, MYOD, and MYHC in a stable *Dmd*^{mdx} iMPC clone and quantification. Arrowheads denote presence of immature PAX7^{+}/MYOD^{-} cells. Error bars denote SD, scale bar, 100 μm.
(H) Timeline of experimental design.
(I) Flow cytometry analysis of *Dmd*^{mdx} iMPCs stained with an antibody recognizing VCAM-1 (right) and an unstained control (left).
(J) VCAM-1 staining of *Dmd*^{mdx} iMPCs generated from FACS-purified VCAM-1^{+} cells after 21 days. Scale bar, 100 μm.
(K) Microscopy images showing GFP expression from the Pax7 locus in *Pax7-nGFP; Dmd*^{mdx} and *Pax7-nGFP; Dmd*$^{mdx-4Cv}$ iMPCs. Scale bar, 100 μm.
(L) Flow cytometry analysis of GFP expression in *Pax7-nGFP; Dmd*^{mdx} iMPCs.
(M) Experimental outline. MPCs, myogenic progenitor cells.
(N) Microscopy images of *Pax7-nGFP; Dmd*^{mdx} MPCs. Scale bar, 100 μm.
(O) Flow cytometry analysis of GFP expression in *Pax7-nGFP; Dmd*^{mdx} MPCs.

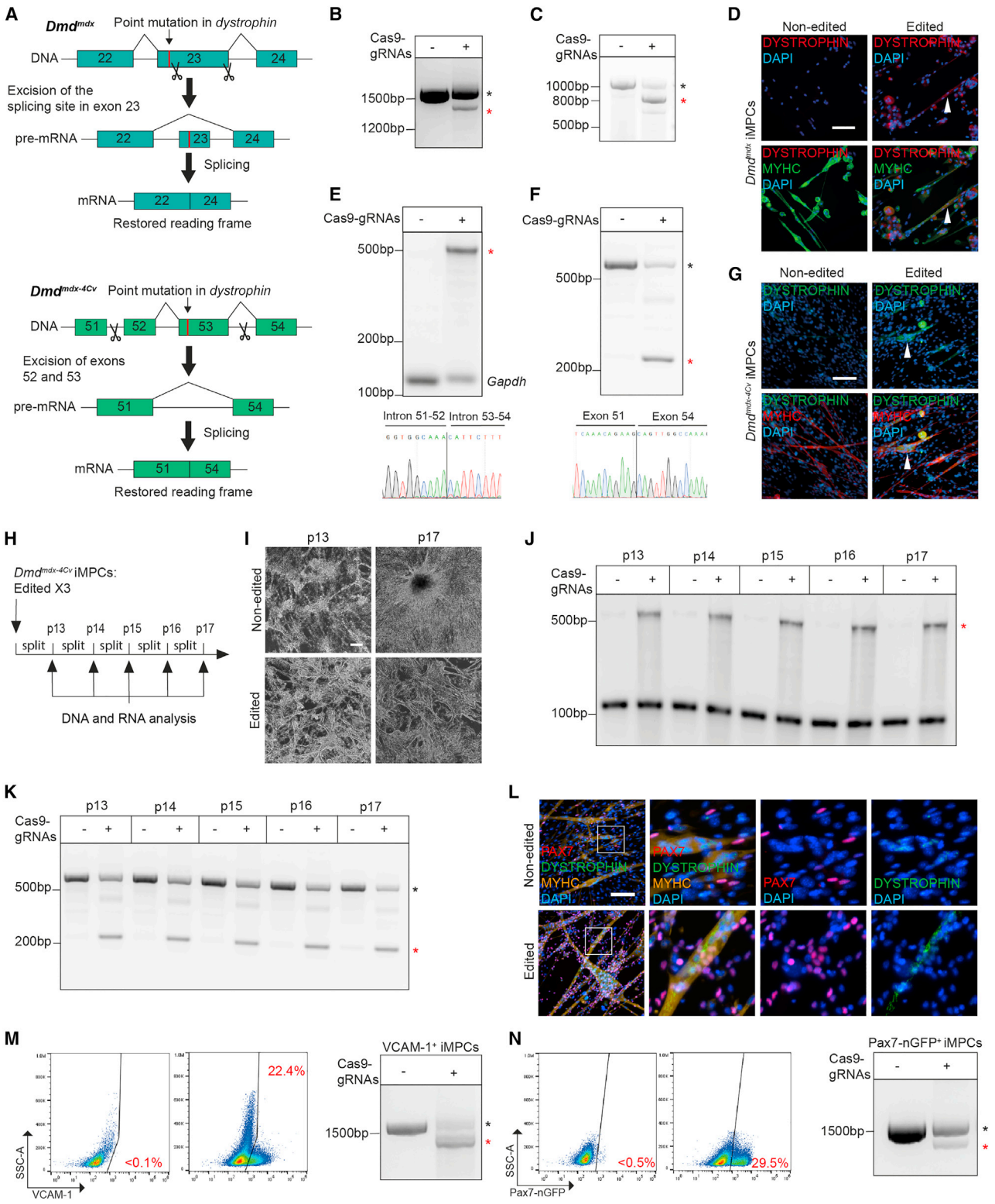

Figure 4. Correction of the *dystrophin* mutation in DMD iMPCs with CRISPR/Cas9

(A) An overview of experimental strategy to correct the *Dmd*^{mdx} and *Dmd*$^{mdx\text{-}4Cv}$ mutation.

(B) PCR analysis for the *Dmd* gene using genomic DNA (gDNA) extracted from non-edited(−) and edited(+) *Dmd*^{mdx} iMPCs. The unedited PCR product size is 1,572 bp, whereas the edited product size is 1,377 bp (black and red asterisks, respectively).

(legend continued on next page)

expression of VCAM-1, an established satellite cell surface marker (Figures 3H and 3I) (Liu et al., 2013). This FACS analysis determined that about 27% of the mononucleated cells in *Dmd*^{mdx} iMPCs were positive for VCAM-1 (Figure 3I). Furthermore, FACS purification of VCAM-1^{+} cells from *Dmd*^{mdx} iMPCs gave rise to a population of VCAM-1^{+} mononucleated cells that could differentiate and form the entire myofiber network of iMPCs within 14–21 days (Figure 3J).

Genetic reporters represent an alternative method to isolate stem cells from heterogeneous cultures and have been widely used to purify satellite cells from skeletal muscles of mice, for example using GFP expression regulated by a Pax7 promoter (Bosnakovski et al., 2008; Sambasivan et al., 2009). Given that Pax7 is widely expressed in *Dmd*^{mdx} iMPCs, we next wished to determine whether a genetic reporter for Pax7 may provide a facile method to isolate stem cells from the heterogeneous iMPC cultures. To this end, we generated *Pax7-nuclear(n)GFP*; *Dmd*^{mdx} or *Dmd*$^{mdx-4Cv}$ MEFs and reprogrammed these cells into iMPCs (Figure 3K). *Pax7-nGFP*; *Dmd*^{mdx} or *Dmd*$^{mdx-4Cv}$ iMPCs could proliferate robustly and contained mononucleated GFP^{+} cells (Figure 3K and 3L). Furthermore, a previous study reported on the generation of myogenic progenitor cells (MPCs) by exposing dissociated muscle fragments isolated from adult mice to F/R/C supplementation (Bar-Nur et al., 2018). In an effort to recapitulate this finding with DMD myogenic cells, we subjected dissociated skeletal muscle fragments from *Pax7-nGFP*; *Dmd*^{mdx} adult mice to F/R/C treatment. Within 2–4 weeks, we were able to generate MPCs harboring contractile myofibers and three-dimensional colonies that proliferated robustly and expressed the nGFP reporter (Figures 3M–3O; Videos S3 and S4). Notably, many of the Pax7-nGFP^{+} cell population of MPCs was also positive for VCAM-1, confirming the validity of either approaches to purify stem cells from MPC and iMPC cultures (Figures S3B). Taken together, these findings establish that DMD iMPCs can proliferate long term *in vitro*, while expressing stem, progenitor, and differentiation cell markers in the absence of DYSTROPHIN expression. Moreover, these progenitor cells can be FACS-purified from the heterogeneous cultures via the cell surface marker VCAM-1 or a *Pax7-nGFP* reporter.

Utilizing gene editing with CRISPR/Cas9 to correct the *dystrophin* mutation in iMPCs

As *Dmd*^{mdx} and *Dmd*$^{mdx-4Cv}$ iMPCs can proliferate long term *in vitro* and produce mature and contractile DYSTROPHIN-negative myofibers, our next goal was to investigate whether gene editing of the *mdx or mdx-4Cv* mutation can restore DYSTROPHIN expression *in vitro*. To achieve this goal, we opted to use an exon skipping-based approach, which was previously shown to correct the *dystrophin* mutation in skeletal muscles of *Dmd*^{mdx} or *Dmd*$^{mdx-4Cv}$ mice (Bengtsson et al., 2017; Long et al., 2016). For *Dmd*^{mdx}, this approach entails excision of the donor splice site of *dystrophin*'s exon 23, which contains the *mdx* mutation and subsequent ligation of exon 22 and 24, thus generating a shorter yet functional DYSTROPHIN protein (Figure 4A) (Long et al., 2016). For

(C) PCR for *Dmd* in cDNA of non-edited(−) and edited(+) *Dmd*^{mdx} iMPCs. The unedited PCR product size is 1,015 bp, whereas the edited product size is 802 bp (black and red asterisks, respectively).
(D) Representative immunofluorescence images for DYSTROPHIN in non-edited and edited *Dmd*^{mdx} iMPCs. White arrowheads point to a DYSTROPHIN-positive myofiber. Scale bar, 100 μm.
(E) Top: *Dmd* PCR for non-edited(−) and edited(+) *Dmd*$^{mdx-4Cv}$ iMPCs. Non-edited cells do not show a PCR product, whereas successful editing leads to a PCR fragment of 492 bp (red asterisk). *Gapdh* was used as a control. Bottom: DNA sequencing reveals excision of exons 52 and 53.
(F) Top: PCR for *Dmd* in cDNA of non-edited(−) and edited(+) *Dmd*$^{mdx-4Cv}$ iMPCs. mRNA from non-edited cells leads to a PCR fragment of 567 bp, whereas editing results in a 237 bp fragment (black and red asterisks, respectively). Bottom: cDNA sequence of edited *Dmd*$^{mdx-4Cv}$ iMPCs reveals ligation of exons 51 and 54.
(G) Immunofluorescence images of non-edited and edited *Dmd*$^{mdx-4Cv}$ iMPCs. A white arrowhead points to a DYSTROPHIN-positive myofiber. Scale bar, 100 μm.
(H) Overview of experimental design.
(I) Brightfield images of non-edited and edited *Dmd*$^{mdx-4Cv}$ iMPCs at passages 13 and 17. Scale bar, 200 μm.
(J) PCR for *Dmd* using gDNA extracted from non-edited(−) and edited(+) *Dmd*$^{mdx-4Cv}$ iMPCs at the indicated passages. Expected edited product size is marked with a red asterisk. The lower band corresponds to a *Gapdh* control.
(K) PCR for *Dmd* in cDNA of non-edited(−) and edited(+) *Dmd*$^{mdx-4Cv}$ iMPCs at the indicated passages. The unedited PCR product is 567 bp, whereas the edited fragment is 237 bp.
(L) Immunofluorescence images of non-edited and edited *Dmd*$^{mdx-4Cv}$ iMPCs at P17. Scale bar, 100 μm.
(M) Left: Flow cytometry analysis for VCAM-1 in *Dmd*^{mdx} iMPCs versus an unstained control (left FACS plot). Right: PCR analysis for the *Dmd* gene in *Dmd*^{mdx} iMPCs established from VCAM-1^{+} sorted cells. The edited PCR product is labeled with a red asterisk.
(N) Left: Flow cytometry analysis for GFP expression in *Pax7-nGFP; Dmd*^{mdx} iMPCs versus *Dmd*^{mdx} iMPCs as negative control (left FACS plot). Right: PCR for the *Dmd* gene in FACS-purified *Pax7-nGFP; Dmd*^{mdx} iMPCs. The edited product is labeled with a red asterisk.

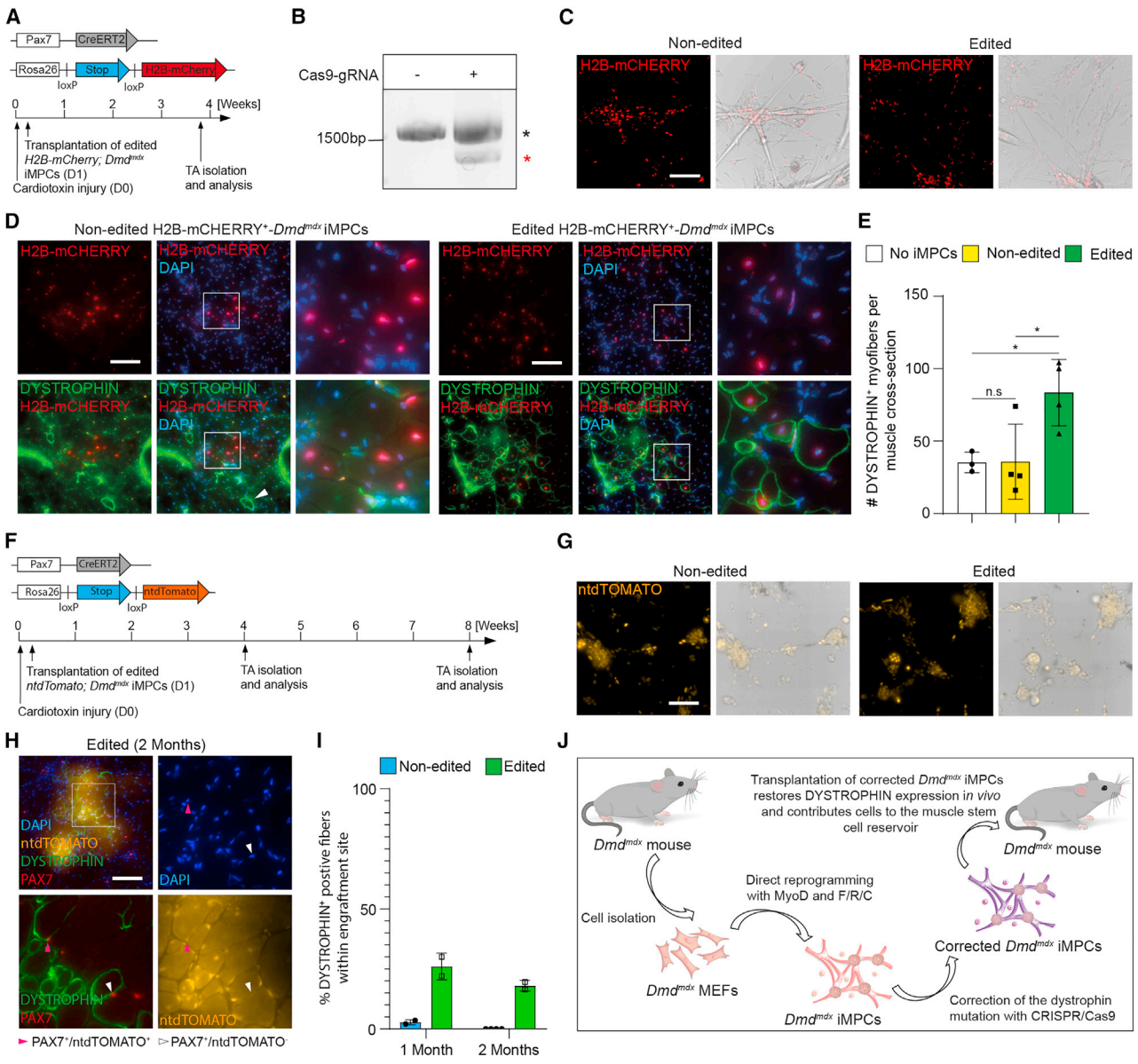

Figure 5. Genetically corrected *Dmd*^{mdx} iMPCs restore DYSTROPHIN expression *in vivo*

(A) An experimental workflow. TA, *Tibialis Anterior*.

(B) PCR for the *Dmd* gene in non-edited(−) or edited(+) *Pax7-CreERT2; R26-LSL-H2B-mCherry-Dmd*^{mdx} iMPCs. The edited PCR product size is 1,377 bp and marked with a red asterisk.

(C) Microscopy images of the indicated *Pax7-CreERT2; Rosa26-LSL-H2B-mCherry-Dmd*^{mdx} iMPCs. Scale bar, 100 μm.

(D) Representative immunofluorescence images of two TA muscle cross-sections engrafted with either 1 million non-edited or edited H2B-mCHERRY^{+}-*Dmd*^{mdx} iMPCs. A white arrowhead points to a rare DYSTROPHIN-positive revertant myofiber. Scale bar, 100 μm.

(E) Quantification of DYSTROPHIN-positive myofibers in the indicated TA muscle cross-sections. Each dot represents a TA muscle of an engrafted *Prkdc*^{scid}; *Dmd*^{mdx} mouse; error bars denote SD. Statistical analysis was performed using ordinary one-way ANOVA. *p $\leq$ 0.05, n.s., not significant.

(F) Top: *Pax7-CreERT2; R26-LSL-ntdTomato* alleles utilized to label Pax7 expressing cells prior to intramuscular transplantation. Bottom: timeline of experimental design.

(G) Representative microscopy images of unedited and edited *Pax7-CreERT2; R26-LSL-ntdTomato, Dmd*^{mdx} iMPCs. Scale bar, 100 μm.

(legend continued on next page)

Dmd$^{mdx-4Cv}$, we utilized a previously reported approach to eliminate the mutation in *dystrophin*'s exon 53 by employing guide RNAs (gRNAs) that excise exons 52 and 53 followed by ligation of exons 51 to 54 (Figure 4A) (Bengtsson et al., 2017).

In our first attempt to correct the *dystrophin* mutation in *Dmd*^{mdx} iMPCs, we engineered a single plasmid consisting of two gRNAs flanking the splice donor site in exon 23, an SpCas9, an mCherry fluorescence reporter, and a hygromycin antibiotic selection cassette. As an alternative method, we also assembled ribonucleoproteins (RNPs), which consisted of SpCas9 and the gRNAs flanking the splice donor site of exon 23. We attempted a lipofectamine-based transfection of the DNA plasmid into *Dmd*^{mdx} iMPCs followed by hygromycin selection. However, we observed low cell transfection, extensive cell death, and inability to expand hygromycin-resistant iMPCs, albeit after repeated attempts, we generated a single partially corrected *Dmd*^{mdx} iMPC clone, which contained edited cells and a few DYSTROPHIN^{+} myofibers (Figures S4A–S4D). Given the low transfection efficiency and poor editing rates documented using the plasmid delivery system, we decided to focus our efforts on the RNP-based system. Transfection of cells with RNPs consistently led to successful editing of *dystrophin* in multiple *Dmd*^{mdx} iMPC clones, even without antibiotic selection (Figures 4B and 4C). Importantly, we detected DYSTROPHIN protein expression in corrected *Dmd*^{mdx} iMPCs (Figures 4D and S4E). Similarly, RNP transfection of *Dmd*$^{mdx-4Cv}$ iMPCs consistently gave rise to partially corrected iMPCs and expression of the DYSTROPHIN protein in several multinucleated myofibers (Figures 4E–4G and S4F).

Due to the heterogeneity of iMPC cultures, we could not decipher whether the gene editing of *Dmd*^{mdx} iMPCs occurred in myogenic progenitors that further differentiated into DYSTROPHIN-positive myofibers, or solely in DYSTROPHIN-negative myofibers that became positive following RNP transfection. This notion is important for cell-based therapy, as gene-corrected progenitors can be utilized for intramuscular transplantation. To investigate this question and as corrected DYSTROPHIN^{+} myofibers are not expandable, we edited *Dmd*$^{mdx-4Cv}$ iMPCs three times to increase the population of edited cells and propagated them for an additional five passages, purposing to decipher whether gene-edited cells persisted in the culture during passaging (Figure 4H). Notably, we detected a gene-edited *dystrophin* band during each consecutive passage at both the DNA and RNA level in addition to DYSTROPHIN protein expression in myofibers (Figures 4I–4L). These findings suggest that the expandable mononucleated cells of DMD iMPCs were successfully edited and maintained corrected cells during passaging.

Finally, to further corroborate that gene editing occurred in the stem cell population of iMPCs, we FACS-purified VCAM-1^{+} progenitors from *Dmd*^{mdx} iMPCs and transfected the mononucleated cells with RNPs 1 day post FACS purification and before any visible myofibers could form (Figures 4M and S4G). Following 11 days of culture, VCAM-1^{+} progenitors gave rise to *Dmd*^{mdx} iMPC cultures consisting of progenitors and myofibers, which were partially edited (Figure 4M). Similarly, we also FACS-purified GFP^{+} cells from *Pax7-nGFP*; *Dmd*^{mdx} iMPCs and 6 h post cell sorting transfected the cells with RNPs (Figure 4N). Following 5 weeks of culture, GFP^{+} cells gave rise to *Pax7-nGFP; Dmd*^{mdx} iMPCs that were partially edited (Figure 4N). Lastly, we successfully edited FACS-purified Pax7-nGFP^{+} cells, which were sorted from *Pax7-nGFP*; *Dmd*^{mdx} MPCs (Figures S4H and S4I).

Corrected DMD iMPCs restore DYSTROPHIN expression *in vivo* and contribute to the muscle stem cell reservoir

Our success in editing the *dystrophin* mutation in the stem cell subsets of DMD iMPCs prompted us to investigate whether corrected DMD iMPCs can efficiently engraft into dystrophic limb muscles and restore DYSTROPHIN expression *in vivo*. To explore this possibility, we utilized *Dmd*^{mdx} iMPCs that also harbor *Pax7-CreERT2; R26-LSL-H2B-mCherry* alleles, which allow labeling of PAX7^{+} cells with nuclear H2B-mCHERRY prior to transplantation (Figures 5A–5C). Utilizing such a fluorescent reporter system was necessary to distinguish between rare DYSTROPHIN-positive revertant myofibers present in the *Dmd*^{mdx} mouse model versus DYSTROPHIN-positive myofibers emanating from cell fusion with corrected DMD iMPCs. To facilitate engraftment of cells, we pre-injured the *Tibialis Anterior* (TA) muscles of immunodeficient *Prkdc*^{scid}; *Dmd*^{mdx} mice with cardiotoxin (CTX) one day prior to cell transplantation (Figure 5A). We further confirmed that *dystrophin* was successfully edited in a subset of H2B-mCHERRY^{+}-*Dmd*^{mdx} iMPCs prior to engraftment (Figure 5B). Next, we injected

(H) Immunofluorescence image of a muscle cross-section demonstrating engraftment of edited *Pax7-CreERT2; R26-LSL-ntdTomato; Dmd*^{mdx} iMPCs two months post transplantation. A pink arrowhead points to a PAX7^{+}/ntdTOMATO^{+} cell in association with a DYSTROPHIN-positive myofiber. The white arrowhead points to an endogenous PAX7^{+}/ntdTOMATO^{-} satellite cell. Scale bar, 200 μm.

(I) Quantification of DYSTROPHIN-positive myofibers within the engraftment area at the indicated time points. Each dot represents one TA muscle of an engrafted *Prkdc*^{scid}; *Dmd*^{mdx} mouse; error bars denote SD.

(J) A summarizing schematic.

non-edited or edited H2B-mCHERRY$^+$-*Dmd*^{mdx} iMPCs into the left and right TA muscles of *Prkdc*^{scid};*Dmd*^{mdx} mice, respectively. At 3.5 weeks post transplantation, TA muscles from both conditions contained myofibers harboring H2B-mCHERRY-positive cells, indicating successful cell fusion of DMD iMPCs with dystrophic muscles (Figures 5D and S5A). Namely, only in muscles engrafted with corrected H2B-mCHERRY$^+$-*Dmd*^{mdx} iMPCs, we could detect distinct clusters of H2B-mCHERRY$^+$ myonuclei in association with DYSTROPHIN-positive myofibers around the injection site (Figures 5D, 5E, S5A, and S5B). Of note, the presence of DYSTROPHIN$^+$ myofibers in non-engrafted TA muscles or those engrafted with non-edited *Dmd*^{mdx} iMPCs was due to naturally occurring revertant DYSTROPHIN-positive myofibers, which are common in the *Dmd*^{mdx} mouse model (Hoffman et al., 1990).

We previously showed that WT iMPCs and MPCs can contribute cells to the muscle stem cell pool *in vivo* (Bar-Nur et al., 2018). To investigate whether DMD myogenic progenitors harbor a similar propensity, we injected *Pax7-nGFP*; *Dmd*^{mdx} MPCs into pre-injured TA muscles of *Prkdc*^{scid}; *Dmd*^{mdx} mice (Figures S5C and S5D). One month post transplantation, TA muscles were harvested, digested, and subjected to Flow cytometry analysis. Remarkably, of the total mononucleated cells in transplanted TA muscles, around 0.8% were Pax7-nGFP$^+$ donor-derived cells (Figure S5E). Moreover, culturing these FACS-purified Pax7-nGFP$^+$ cells in conventional myoblast medium successfully generated myoblasts expressing the Pax7 reporter (Figure S5F). These findings suggest that engrafted DMD myogenic progenitors remained as stem cells *in vivo*, indicating that they may harbor long-term regeneration potential. Building upon this observation, we opted to assess whether engraftment of gene-edited DMD iMPCs can lead to long-term DYSTROPHIN restoration as well as a contribution of donor-derived cells to the muscle stem cell pool *in vivo*. To this end, we transplanted edited and non-edited *Dmd*^{mdx} iMPCs, which carry a *Pax7-CreERT2; R26-LSL-ntdTomato* reporter into CTX pre-injured TA muscles of *Prkdc*^{scid}; *Dmd*^{mdx} mice and harvested the muscles either 1 or 2 months post transplantation (Figures 5F, 5G, S5G–S5J). We detected approximately the same number of DYSTROPHIN$^+$ myofibers after 1 or 2 months, suggesting long-term restoration (Figures 5H and 5I). Furthermore, we inspected the injection area for PAX7$^+$ mononucleated cells in association with DYSTROPHIN$^+$ myofibers that also carry the ntdTOMATO label and detected PAX7$^+$/ntdTOMATO$^+$ at the expected anatomical location of satellite cells, suggesting contribution to the muscle stem cell pool (Figures 5H and S5K). Of note, mCHERRY$^+$ or ntdTOMATO$^+$ myonuclei in muscle fibers may be donor derived or represent endogenous myonuclei that are H2B-mCHERRY$^+$ or ntdTOMATO$^+$ due to protein shuttling in multinucleated myofibers (Masschelein et al., 2020; Taylor-Weiner et al., 2020); although, all PAX7$^+$/ntdTOMATO$^+$ mononucleated cells are expected to be donor-derived iMPCs. Altogether, the transplantation trials establish that corrected *Dmd*^{mdx} iMPCs can engraft *in vivo* and restore DYSTROPHIN expression in dystrophic limb muscles of *Prkdc*^{scid}; *Dmd*^{mdx} mice. Moreover, these cells can remain as stem cells in recipient muscles and contribute to the satellite cell reservoir.

DISCUSSION

In this study, we report on the generation of highly proliferative myogenic progenitors from the *Dmd*^{mdx} and *Dmd*$^{mdx-4Cv}$ mouse models by direct reprogramming of fibroblasts via MyoD overexpression in concert with F/R/C treatment, or exposure of dissociated muscle fragments solely to F/R/C supplementation. DMD iMPCs proliferate extensively, express canonical satellite cell markers, and can give rise to highly contractile DYSTROPHIN-negative myofibers. Utilizing an exon skipping-based approach with CRISPR/Cas9, we demonstrate successful editing of the *dystrophin* mutation *in vitro*, most notably in the stem cell subset of DMD iMPCs. Last, we report on the restoration of DYSTROPHIN expression *in vivo* in dystrophic muscles via engraftment of genetically corrected DMD iMPCs and determine that engrafted cells contribute to the muscle stem cell pool (Figure 5J).

In recent years, several studies have reported on genetic correction of myogenic cells utilizing various genome engineering approaches. For example, *Dmd*^{mdx} satellite cells and myoblasts have been successfully transfected and corrected *in vitro* and were shown to restore DYSTROPHIN expression *in vivo* (Matre et al., 2019; Tabebordbar et al., 2016; Zhu et al., 2017). Another study successfully trialed an introduction of a human artificial chromosome carrying the *DYSTROPHIN* gene into DMD patient fibroblasts prior to reprogramming into induced pluripotent stem cells (iPSCs) and subsequent differentiation into corrected myogenic precursors (Choi et al., 2016). Similarly, CRISPR/Cas9-corrected human DMD iPSCs were differentiated into myogenic cells via overexpression of MyoD and efficiently restored DYSTROPHIN expression in limb muscles of dystrophic mice (Young et al., 2016). It will be of further interest to compare these different models with respect to their efficiency in restoring DYSTROPHIN expression *in vivo* as well as their potential to contribute donor-derived cells to the muscle stem cell reservoir.

Correction of genetic mutations via genome engineering in conjunction with cell transplantation could provide a powerful tool to treat a plethora of genetic diseases. For skeletal muscle tissue, major obstacles still exist for this

approach to succeed, including reduced engraftment potential of primary myoblasts, poor migration of transplanted cells, or cell death of donor-derived myogenic cells in muscles. Different approaches have been established in recent years to address a few of these hurdles, each carrying respective advantages and disadvantages (Domenig et al., 2020; Judson and Rossi, 2020). Direct reprogramming of somatic cells into activated satellite-like cells may address a few of these limitations, namely, the long-term expansion necessary to produce a sufficient number of transplanted cells as well as enhanced engraftment capacities in comparison with other myogenic cell types. However, expediating the migration of cells across skeletal muscle tissue for sufficient engraftment still presents a major challenge. To address this limitation, it will be of interest to assess whether high-proximity injections of iMPCs may assist in producing a sufficient quantity of DYSTROPHIN-positive myofibers deemed necessary for therapeutic relevancy (Skuk et al., 2007). Additionally, to fully determine the competency of genetically corrected DMD iMPCs, it will be of interest to assess their potential to sustain a repeated injury assay, as previously demonstrated for WT iMPCs (Bar-Nur et al., 2018).

Cell-based therapy is one of several proposed approaches to restore DYSTROPHIN expression in skeletal muscles of DMD patients. Whereas this approach is not expected to provide systemic restoration of DYSTROPHIN, it is plausible that even restoration of DYSTROPHIN in small muscles, such as finger muscles, may improve a patient's quality of life, as it may enable controlling digital devices. Development of systemic approaches to restore DYSTROPHIN expression in less accessible muscles such as the heart or diaphragm are still highly warranted. To this end, adeno-associated viruses (AAVs), encoding for micro-dystrophin or CRISPR/Cas9 and gRNAs, may provide a superior systemic therapeutic approach (Furrer and Handschin, 2019). Accordingly, successful gene editing of skeletal and cardiac muscles *in vivo* has been demonstrated using CRISPR/Cas9 in mice and dogs, exhibiting extensive DYSTROPHIN restoration in myofibers (Amoasii et al., 2018; Long et al., 2016; Nelson et al., 2016; Tabebordbar et al., 2016). However, challenges still face this therapeutic approach in humans, namely, an immunological reaction against AAVs may preclude this method from gaining therapeutic adoption. Furthermore, given the relatively high turn-over rate of skeletal muscle tissue, long-term therapy may necessitate gene editing of mutated satellite cells *in vivo*, which was initially deemed ineffective using AAVs; although, recent studies show feasibility (Arnett et al., 2014; Goldstein et al., 2019; Nance et al., 2019; Tabebordbar et al., 2016).

Finally, we report here on generation of iMPCs from two DMD mouse models, similar to recent reports on generation of mouse iMPCs from WT somatic cells (Bar-Nur et al., 2018; Ito et al., 2017; Sato et al., 2019). Utilizing a direct reprogramming approach, one study further reported on the generation of human iMPCs; however, these progenitors were only partially characterized (Sato et al., 2019). As such, it is still of paramount interest to seek novel means to reprogram human somatic cells directly into *bona fide* expandable iMPCs. With success, further research will be warranted to assess production of iMPCs from human DMD patients, paving the way to potentially trial genetic correction and autologous engraftment of directly reprogrammed iMPCs.

EXPERIMENTAL PROCEDURES

Details on reagents, antibodies, transcriptional analysis, gene editing, and *in vivo* engraftment assays can be found in the supplemental information.

Mouse models

The mouse strains reported in this study were gender group housed with standard food and water *ad libitum* and kept under specific-pathogen-free (SPF)-like conditions. Animal handling and experiments were carried out in accordance with the Swiss Federal Law on Animal Protection, and respective protocols were approved by the Cantonal Animal Welfare Committee (protocol number ZH177-18). The following mouse strains were obtained from Jackson Laboratories and used in this study: C57BL/10ScSn-*Dmd*^{mdx}/J (Stock No: 001,801); B6Ros.Cg-*Dmd*$^{mdx-4Cv}$/J (Stock No: 002,378); B10ScSn.Cg-*Prkdc*^{scid} *Dmd*^{mdx}/J (Stock No: 018,018); B6; 129S- *Gt(ROSA)*$^{26Sortm1.1Ksvo}$/J (Stock No: 023,139); B6.Cg-*Pax7*$^{tm1(cre/ERT2)Gaka}$/J (Stock No: 017,763). B6.Cg-*Gt(ROSA)26Sor*$^{tm75.1(CAG-tdTomato*)Hze}$/J (Stock No: 025,106). Additionally, previously reported *Tg:Pax7-nGFP/C57BL6;DBA2* mice were used and crossed with the various DMD mouse strains (Sambasivan et al., 2009). Male and female, 13–32-week-old B10ScSn.Cg-*Prkdc*^{scid} *Dmd*^{mdx}/J mice were used as recipients for the *in vivo* transplantation experiments.

Reprogramming of MEFs into iMPCs

A modification of a recently published reprogramming method was used in this study (Bar-Nur et al., 2018). In brief, transduced MEFs were selected with 1–2 ug/mL Puromycin (Cat. #A1113803, Thermo Fisher Scientific) alone or with 0.5 1ug/mL Neomycin (Cat. #4727878001, Sigma-Aldrich). The cells were cultured in "iMPCs medium" supplemented with F/R/C and 2 μg/mL dox (Cat. #D9891, Sigma-Aldrich) for 7–14 days, followed by dox withdrawal and further culture in "iMPC medium" supplemented with F/R/C for several days. Control MEFs were cultured in parallel only with "iMPC medium." For reprogramming of MEFs with MyoD overexpression alone, cells were cultured for 7–14 days in "iMPC medium" supplemented with 2 μg/mL dox (Cat. #D9891, Sigma-Aldrich) followed by culturing cells for several days only in "iMPC medium." For the experiments described in this work, MEFs (passages 3–5) were plated onto 6-well plates at 100,000–200,000 cells/well confluency for successful reprogramming.

Data and code availability

The RNA-seq datasets generated in this study are available in the Gene Expression Omnibus (GEO) repository under accession number GEO: GSE164599. Myoblast RNA-seq datasets were previously reported (Kim et al., 2021)

SUPPLEMENTAL INFORMATION

Supplemental information can be found online at https://doi.org/10.1016/j.stemcr.2021.12.003.

AUTHOR CONTRIBUTIONS

O. Bar-Nur and S. Domenig conceptualized the study, designed the experiments, interpreted the results, and wrote the manuscript. O. Bar-Nur supervised the study. S. Domenig performed most experiments and analysis of results. N. Bundschuh assisted with FACS, cell transplantation, and lentiviral production. A. Lenardič reprogrammed, characterized, and edited the *Dmd*$^{mdx-4Cv}$ iMPCs. A. Ghosh performed the processing and analysis of the RNA-seq data. I. Kim assisted with analyzing the RNA-seq data in addition to maintaining and labeling iMPCs. X. Qabrati assisted in conducting the VCAM-1 FACS experiments, and G. D'Hulst performed the Western blot analysis of *Dmd*$^{mdx-4Cv}$ iMPCs.

CONFLICT OF INTERESTS

The authors declare no competing interests.

ACKNOWLEDGMENTS

We wish to thank Dr. Bruno Di Stefano as well as members of the Regenerative and Movement Biology laboratory for their constructive comments and feedback. We are grateful to Dr. Shahragim Tajbakhsh for providing the *Pax7-nGFP* mouse strain and Dr. Konrad Hochedlinger for sharing the *pLV-tetO-MyoD* and *pLV-M2rtTA* plasmids. We also wish to thank Dr. Katrien De Bock for fruitful discussions, Joel Zvick for support with microscopy, and Valerie Wiesbauer for assisting with the generation of MPCs. We acknowledge the use of the Functional Genomics Center Zurich (FGCZ) facility and are grateful to their staff members for their assistance. We also wish to thank SciArtWork for their help with preparation of graphical images. This work was supported by startup funds from ETH Zurich and an Eccellenza Grant (PCEGP3_187009) from the Swiss National Science Foundation to O.B.-N. Other support to the Bar-Nur lab includes grants from The Good Food Institute Foundation, The Novartis Foundation for Medical-Biological Research, The Helmut Horten Foundation, and the National Centre of Competence in Research (NCCR) Robotics of the Swiss National Science Foundation.

Received: March 18, 2021
Revised: December 6, 2021
Accepted: December 7, 2021
Published: January 6, 2022

REFERENCES

Amoasii, L., Hildyard, J.C.W., Li, H., Sanchez-Ortiz, E., Mireault, A., Caballero, D., Harron, R., Stathopoulou, T.R., Massey, C., Shelton, J.M., et al. (2018). Gene editing restores dystrophin expression in a canine model of Duchenne muscular dystrophy. Science *362*, 86–91.

Arnett, A.L., Konieczny, P., Ramos, J.N., Hall, J., Odom, G., Yablonka-Reuveni, Z., Chamberlain, J.R., and Chamberlain, J.S. (2014). Adeno-associated viral (AAV) vectors do not efficiently target muscle satellite cells. Mol. Ther. Methods Clin. Dev. *1*, 14038.

Bar-Nur, O., Gerli, M.F.M., Di Stefano, B., Almada, A.E., Galvin, A., Coffey, A., Huebner, A.J., Feige, P., Verheul, C., Cheung, P., et al. (2018). Direct reprogramming of mouse fibroblasts into functional skeletal muscle progenitors. Stem Cell Rep. *10*, 1505–1521.

Ben-David, U., and Benvenisty, N. (2011). The tumorigenicity of human embryonic and induced pluripotent stem cells. Nat. Rev. Cancer *11*, 268–277.

Bengtsson, N.E., Hall, J.K., Odom, G.L., Phelps, M.P., Andrus, C.R., Hawkins, R.D., Hauschka, S.D., Chamberlain, J.R., and Chamberlain, J.S. (2017). Muscle-specific CRISPR/Cas9 dystrophin gene editing ameliorates pathophysiology in a mouse model for Duchenne muscular dystrophy. Nat. Commun. *8*, 14454.

Bosnakovski, D., Xu, Z., Li, W., Thet, S., Cleaver, O., Perlingeiro, R.C., and Kyba, M. (2008). Prospective isolation of skeletal muscle stem cells with a Pax7 reporter. Stem Cells *26*, 3194–3204.

Bulfield, G., Siller, W.G., Wight, P.A., and Moore, K.J. (1984). X chromosome-linked muscular dystrophy (mdx) in the mouse. Proc. Natl. Acad. Sci. U S A *81*, 1189–1192.

Chal, J., Oginuma, M., Al Tanoury, Z., Gobert, B., Sumara, O., Hick, A., Bousson, F., Zidouni, Y., Mursch, C., Moncuquet, P., et al. (2015). Differentiation of pluripotent stem cells to muscle fiber to model Duchenne muscular dystrophy. Nat. Biotechnol. *33*, 962–969.

Chapman, V.M., Miller, D.R., Armstrong, D., and Caskey, C.T. (1989). Recovery of induced mutations for X chromosome-linked muscular dystrophy in mice. Proc. Natl. Acad. Sci. U S A *86*, 1292–1296.

Choi, I.Y., Lim, H., Estrellas, K., Mula, J., Cohen, T.V., Zhang, Y., Donnelly, C.J., Richard, J.P., Kim, Y.J., Kim, H., et al. (2016). Concordant but varied phenotypes among Duchenne muscular dystrophy patient-specific myoblasts derived using a human iPSC-based model. Cell Rep. *15*, 2301–2312.

Comai, G., and Tajbakhsh, S. (2014). Molecular and cellular regulation of skeletal myogenesis. Curr. Top Dev. Biol. *110*, 1–73.

Darabi, R., Arpke, R.W., Irion, S., Dimos, J.T., Grskovic, M., Kyba, M., and Perlingeiro, R.C. (2012). Human ES- and iPS-derived myogenic progenitors restore DYSTROPHIN and improve contractility upon transplantation in dystrophic mice. Cell Stem Cell *10*, 610–619.

Davis, R.L., Weintraub, H., and Lassar, A.B. (1987). Expression of a single transfected cDNA converts fibroblasts to myoblasts. Cell *51*, 987–1000.

Domenig, S.A., Palmer, A.S., and Bar-Nur, O. (2020). Stem cell-based and tissue engineering approaches for skeletal muscle repair. In Organ Tissue Engineering, D. Eberli, S.J. Lee, and A. Traweger, eds. (Springer International Publishing), pp. 1–62.

Dowling, J.J., Weihl, C.C., and Spencer, M.J. (2021). Molecular and cellular basis of genetically inherited skeletal muscle disorders. Nat. Rev. Mol. Cell Biol. *22*, 713–732.

Furrer, R., and Handschin, C. (2019). Muscle wasting diseases: novel targets and treatments. Annu. Rev. Pharmacol. Toxicol. *59*, 315–339.

Goldstein, J.M., Tabebordbar, M., Zhu, K., Wang, L.D., Messemer, K.A., Peacker, B., Ashrafi Kakhki, S., Gonzalez-Celeiro, M., Shwartz, Y., Cheng, J.K.W., et al. (2019). In situ modification of tissue stem and progenitor cell genomes. Cell Rep. *27*, 1254–1264.e7.

Hicks, M.R., Hiserodt, J., Paras, K., Fujiwara, W., Eskin, A., Jan, M., Xi, H., Young, C.S., Evseenko, D., Nelson, S.F., et al. (2018). ERBB3 and NGFR mark a distinct skeletal muscle progenitor cell in human development and hPSCs. Nat. Cell Biol. *20*, 46–57.

Hoffman, E.P., Brown, R.H., Jr., and Kunkel, L.M. (1987). Dystrophin: the protein product of the Duchenne muscular dystrophy locus. Cell *51*, 919–928.

Hoffman, E.P., Morgan, J.E., Watkins, S.C., and Partridge, T.A. (1990). Somatic reversion/suppression of the mouse mdx phenotype in vivo. J. Neurol. Sci. *99*, 9–25.

Ito, N., Kii, I., Shimizu, N., Tanaka, H., and Takeda, S. (2017). Direct reprogramming of fibroblasts into skeletal muscle progenitor cells by transcription factors enriched in undifferentiated subpopulation of satellite cells. Sci. Rep. *7*, 8097.

Judson, R.N., and Rossi, F.M.V. (2020). Towards stem cell therapies for skeletal muscle repair. NPJ Regen. Med. *5*, 10.

Kim, I., Ghosh, A., Bundschuh, N., Hinte, L., von Meyenn, F., and Bar-Nur, O. (2021). Integrative molecular roadmap for direct conversion of fibroblasts into myocytes and myogenic progenitor cells. bioRxiv https://doi.org/10.1101/2021.08.20.457151.

Koenig, M., Hoffman, E.P., Bertelson, C.J., Monaco, A.P., Feener, C., and Kunkel, L.M. (1987). Complete cloning of the Duchenne muscular dystrophy (DMD) cDNA and preliminary genomic organization of the DMD gene in normal and affected individuals. Cell *50*, 509–517.

Kuang, S., Kuroda, K., Le Grand, F., and Rudnicki, M.A. (2007). Asymmetric self-renewal and commitment of satellite stem cells in muscle. Cell *129*, 999–1010.

Li, H.L., Fujimoto, N., Sasakawa, N., Shirai, S., Ohkame, T., Sakuma, T., Tanaka, M., Amano, N., Watanabe, A., Sakurai, H., et al. (2015). Precise correction of the dystrophin gene in duchenne muscular dystrophy patient induced pluripotent stem cells by TALEN and CRISPR-Cas9. Stem Cell Reports *4*, 143–154.

Liu, L., Cheung, T.H., Charville, G.W., Hurgo, B.M., Leavitt, T., Shih, J., Brunet, A., and Rando, T.A. (2013). Chromatin modifications as determinants of muscle stem cell quiescence and chronological aging. Cell Rep. *4*, 189–204.

Long, C., Amoasii, L., Mireault, A.A., McAnally, J.R., Li, H., Sanchez-Ortiz, E., Bhattacharyya, S., Shelton, J.M., Bassel-Duby, R., and Olson, E.N. (2016). Postnatal genome editing partially restores dystrophin expression in a mouse model of muscular dystrophy. Science *351*, 400–403.

Masschelein, E., D'Hulst, G., Zvick, J., Hinte, L., Soro-Arnaiz, I., Gorski, T., von Meyenn, F., Bar-Nur, O., and De Bock, K. (2020). Exercise promotes satellite cell contribution to myofibers in a load-dependent manner. Skelet Muscle *10*, 21.

Matre, P.R., Mu, X., Wu, J., Danila, D., Hall, M.A., Kolonin, M.G., Darabi, R., and Huard, J. (2019). CRISPR/Cas9-Based dystrophin restoration reveals a novel role for dystrophin in bioenergetics and stress resistance of muscle progenitors. Stem Cells *37*, 1615–1628.

Montarras, D., Morgan, J., Collins, C., Relaix, F., Zaffran, S., Cumano, A., Partridge, T., and Buckingham, M. (2005). Direct isolation of satellite cells for skeletal muscle regeneration. Science *309*, 2064–2067.

Murphy, M.M., Lawson, J.A., Mathew, S.J., Hutcheson, D.A., and Kardon, G. (2011). Satellite cells, connective tissue fibroblasts and their interactions are crucial for muscle regeneration. Development *138*, 3625–3637.

Nance, M.E., Shi, R., Hakim, C.H., Wasala, N.B., Yue, Y., Pan, X., Zhang, T., Robinson, C.A., Duan, S.X., Yao, G., et al. (2019). AAV9 edits muscle stem cells in normal and dystrophic adult mice. Mol. Ther. *27*, 1568–1585.

Nelson, C.E., Hakim, C.H., Ousterout, D.G., Thakore, P.I., Moreb, E.A., Castellanos Rivera, R.M., Madhavan, S., Pan, X., Ran, F.A., Yan, W.X., et al. (2016). In vivo genome editing improves muscle function in a mouse model of Duchenne muscular dystrophy. Science *351*, 403–407.

Ousterout, D.G., Kabadi, A.M., Thakore, P.I., Majoros, W.H., Reddy, T.E., and Gersbach, C.A. (2015). Multiplex CRISPR/Cas9-based genome editing for correction of dystrophin mutations that cause Duchenne muscular dystrophy. Nat. Commun. *6*, 6244.

Partridge, T. (2000). The current status of myoblast transfer. Neurol. Sci. *21*, S939–S942.

Polo, J.M., Anderssen, E., Walsh, R.M., Schwarz, B.A., Nefzger, C.M., Lim, S.M., Borkent, M., Apostolou, E., Alaei, S., Cloutier, J., et al. (2012). A molecular roadmap of reprogramming somatic cells into iPS cells. Cell *151*, 1617–1632.

Quarta, M., Brett, J.O., DiMarco, R., De Morree, A., Boutet, S.C., Chacon, R., Gibbons, M.C., Garcia, V.A., Su, J., Shrager, J.B., et al. (2016). An artificial niche preserves the quiescence of muscle stem cells and enhances their therapeutic efficacy. Nat. Biotechnol. *34*, 752–759.

Sacco, A., Doyonnas, R., Kraft, P., Vitorovic, S., and Blau, H.M. (2008). Self-renewal and expansion of single transplanted muscle stem cells. Nature *456*, 502–506.

Sambasivan, R., Gayraud-Morel, B., Dumas, G., Cimper, C., Paisant, S., Kelly, R.G., and Tajbakhsh, S. (2009). Distinct regulatory cascades govern extraocular and pharyngeal arch muscle progenitor cell fates. Dev. Cell *16*, 810–821.

Sato, T., Higashioka, K., Sakurai, H., Yamamoto, T., Goshima, N., Ueno, M., and Sotozono, C. (2019). Core transcription factors promote induction of PAX3-positive skeletal muscle stem cells. Stem Cell Rep. *13*, 352–365.

Sherwood, R.I., Christensen, J.L., Conboy, I.M., Conboy, M.J., Rando, T.A., Weissman, I.L., and Wagers, A.J. (2004). Isolation of adult mouse myogenic progenitors: functional heterogeneity of cells within and engrafting skeletal muscle. Cell *119*, 543–554.

Skuk, D. (2004). Myoblast transplantation for inherited myopathies: a clinical approach. Expert Opin. Biol. Ther. *4*, 1871–1885.

Skuk, D., Goulet, M., Roy, B., Piette, V., Cote, C.H., Chapdelaine, P., Hogrel, J.Y., Paradis, M., Bouchard, J.P., Sylvain, M., et al. (2007). First test of a "high-density injection" protocol for myogenic cell transplantation throughout large volumes of muscles in a Duchenne muscular dystrophy patient: eighteen months follow-up. Neuromuscul. Disord. *17*, 38–46.

Skuk, D., and Tremblay, J.P. (2014). Clarifying misconceptions about myoblast transplantation in myology. Mol. Ther. *22*, 897–898.

Tabebordbar, M., Zhu, K., Cheng, J.K.W., Chew, W.L., Widrick, J.J., Yan, W.X., Maesner, C., Wu, E.Y., Xiao, R., Ran, F.A., et al. (2016). In vivo gene editing in dystrophic mouse muscle and muscle stem cells. Science *351*, 407–411.

Taylor-Weiner, H., Grigsby, C.L., Ferreira, D.M.S., Dias, J.M., Stevens, M.M., Ruas, J.L., and Teixeira, A.I. (2020). Modeling the transport of nuclear proteins along single skeletal muscle cells. Proc. Natl. Acad. Sci. U S A *117*, 2978–2986.

Xi, H., Langerman, J., Sabri, S., Chien, P., Young, C.S., Younesi, S., Hicks, M., Gonzalez, K., Fujiwara, W., Marzi, J., et al. (2020). A human skeletal muscle atlas identifies the trajectories of stem and progenitor cells across development and from human pluripotent stem cells. Cell Stem Cell *27*, 158–176.e10.

Xu, X., Wilschut, K.J., Kouklis, G., Tian, H., Hesse, R., Garland, C., Sbitany, H., Hansen, S., Seth, R., Knott, P.D., et al. (2015). Human satellite cell transplantation and regeneration from diverse skeletal muscles. Stem Cell Rep. *5*, 419–434.

Yiu, E.M., and Kornberg, A.J. (2015). Duchenne muscular dystrophy. J. Paediatr. Child Health *51*, 759–764.

Young, C.S., Hicks, M.R., Ermolova, N.V., Nakano, H., Jan, M., Younesi, S., Karumbayaram, S., Kumagai-Cresse, C., Wang, D., Zack, J.A., et al. (2016). A single CRISPR-Cas9 deletion strategy that targets the majority of DMD patients restores dystrophin function in hiPSC-derived muscle cells. Cell Stem Cell *18*, 533–540.

Zhang, Y., Li, H., Min, Y.L., Sanchez-Ortiz, E., Huang, J., Mireault, A.A., Shelton, J.M., Kim, J., Mammen, P.P.A., Bassel-Duby, R., et al. (2020). Enhanced CRISPR-Cas9 correction of Duchenne muscular dystrophy in mice by a self-complementary AAV delivery system. Sci. Adv. *6*, eaay6812.

Zhu, P., Wu, F., Mosenson, J., Zhang, H., He, T.C., and Wu, W.S. (2017). CRISPR/Cas9-Mediated genome editing corrects dystrophin mutation in skeletal muscle stem cells in a mouse model of mscle dystrophy. Mol. Ther. Nucleic Acids *7*, 31–41.